

Integrated plasma and urine metabolomics coupled with HPLC/QTOF-MS and chemometric analysis on potential biomarkers in liver injury and hepatoprotective effects of Er-Zhi-Wan

Weifeng Yao · Haiwei Gu · Jiangjiang Zhu · Gregory Barding · Haibo Cheng · Beihua Bao · Li Zhang · Anwei Ding · Wei Li

Received: 25 June 2014 / Revised: 12 August 2014 / Accepted: 5 September 2014 / Published online: 23 September 2014
© Springer-Verlag Berlin Heidelberg 2014

Abstract Metabolomics techniques are the comprehensive assessment of endogenous metabolites in a biological system and may provide additional insight into the molecular mechanisms. Er-Zhi-Wan (EZW) is a traditional Chinese medicine formula, which contains *Fructus Ligustri Lucidi*

(FLL) and *Herba Ecliptae* (HE). EZW is widely used to prevent and treat various liver injuries through the nourishment of the liver. However, the precise molecular mechanism of hepatoprotective effects has not been comprehensively explored. Here, an integrated metabolomics strategy was designed to assess the effects and possible mechanisms of EZW against carbon tetrachloride-induced liver injury, a commonly used model of both acute and chronic liver intoxication. High-performance chromatography/quadrupole time-of-flight mass spectrometry (HPLC/QTOF-MS) combined with chemometric approaches including principal component analysis (PCA) and partial least squares-discriminant analysis (PLS-DA) were used to discover differentiating metabolites in metabolomics data of rat plasma and urine. Results indicate six differentiating metabolites, tryptophan, sphinganine, tetrahydrocorticosterone, pipercolic acid, L-2-amino-3-oxobutanoic acid and phosphoribosyl pyrophosphate, in the positive mode. Functional pathway analysis revealed that the alterations in these metabolites were associated with tryptophan metabolism, sphingolipid metabolism, steroid hormone biosynthesis, lysine degradation, glycine, serine and threonine metabolism, and pentose phosphate pathway. Of note, EZW has a potential pharmacological effect, which might be through regulating multiple perturbed pathways to the normal state. Our findings also showed that the robust integrated metabolomics techniques are promising for identifying more biomarkers and pathways and helping to clarify the function mechanisms of traditional Chinese medicine.

Electronic supplementary material The online version of this article (doi:10.1007/s00216-014-8169-x) contains supplementary material, which is available to authorized users.

W. Yao · B. Bao · L. Zhang · A. Ding · W. Li
College of Pharmacy, Nanjing University of Chinese Medicine,
210023 Nanjing, Jiangsu, China

W. Yao · H. Gu · J. Zhu · G. Barding
Northwest Metabolomics Research Center, Department of
Anesthesiology and Pain Medicine, University of Washington,
Seattle, WA 98109, USA

H. Cheng
Jiangsu Engineering Laboratory for Research and Industrialization of
Empirical Formulae, Nanjing University of Chinese Medicine,
210023 Nanjing, Jiangsu, China

B. Bao · L. Zhang (✉) · A. Ding (✉)
Jiangsu Key Laboratory for Traditional Chinese Medicine Formulae
Research, Nanjing University of Chinese Medicine, 210023 Nanjing,
Jiangsu, China
e-mail: zhangliguanxiong@163.com
e-mail: awding105@163.com

H. Gu
Jiangxi Key Laboratory for Mass Spectrometry and Instrumentation,
East China Institute of Technology, 330013 Nanchang, Jiangxi,
China

G. Barding
Department of Chemistry and Biochemistry, California State
Polytechnic University, Pomona, CA 91768, USA

Keywords Integrated metabolomics · Er-Zhi-Wan (EZW) · Hepatoprotective · HPLC/QTOF-MS · Chemometrics

Introduction

Metabolomics has emerged as a powerful approach in systems biology, focusing on a holistic investigation of the small molecular response of living systems to external stimuli, based on global metabolite profiles in biological samples such as plasma, urine, or tissue [1]. Metabolite profiling has enormous potential for the characterization of pathological states in animals [2] and humans [3], as well as providing diagnostic information and presenting mechanistic insight into biochemical effects of drugs [4, 5]. Metabolomics is also an ideal tool to bridge the gap between traditional Chinese medicine (TCM) and molecular pharmacology, partially shedding light on the interacting mechanism between herbal medicine and organism [6–8]. Several groups reported the application of metabolomics of TCM focused on understanding the pathophysiology and assisting in the liver injury or liver diseases [9, 10].

Er-Zhi-Wan (EZW), a famous traditional Chinese formulation firstly recorded in “Yi Bian” written in the Ming Dynasty, contains two herbs viz. *Fructus Ligustri Lucidi* (FLL) and *Herba Ecliptae* (HE). This formulation possesses the actions of tonifying the liver and kidney yin, nourishing body’s essential fluid, and arresting hemorrhage [11]. Pharmacological results indicated that EZW could have the abilities of being hepatoprotective [12], anti-aging [13], activating the estrogenic response [14], and anti-osteoporosis [15]. In our research group, the hepatoprotective property of EZW on the mice liver was determined by the activity determination of serum alanine aminotransferase (ALT) and aspirate aminotransferase (AST), superoxide dismutase (SOD), malondialdehyde (MDA), and the hepatic pathological changes following the treatment [16], indicating the significant recovery action of EZW. In the Pharmacopoeia of the People’s Republic of China [11], the main compounds of EZW, specnuezhenide, wedelolactone, and oleanolic acid, were used to control the quality of FLL, HE, and EZW, respectively. Specnuezhenide is a water-soluble biologically active compound for protecting the natural killer cytotoxicity from inhibition induced by cyclophosphamide and dexamethasone [17]. There was also a report of isolated wedelolactone from HE on suppressing LPS-induced caspase-11 expression by directly inhibiting the IKK Complex, which was tested under in vitro conditions on HeLa cells [18]. Oleanolic acid provides protection against experimental hepatic injury in rats and has been used as an oral remedy for human liver dysfunction [19, 20]. Pretreatment with oleanolic acid also considerably decreases augmentation of serum ALT activity and hepatic centrilobular necrosis induced by chemical hepatotoxicants in mice [21, 22]. However, the action mechanism of the overall effect of EZW has not been studied.

To further investigate the hepatoprotective effect and mechanism of EZW, acute liver injury in rats was induced

by the hepatotoxicant CCl_4 that produces acute liver injury in rodents [23–25]. In recent years, many metabolomics investigators have entered the field of hepatobiliary disease and a considerable volume of publications has appeared [26–28]. The aim of the present study was to find metabolite biomarkers to increase the understanding of the hepatoprotective properties of EZW for the first time. Therefore, a novel strategy for integrated plasma and urine metabolomics was described in this paper based on high-performance chromatography/quadrupole time-of-flight mass spectrometry (HPLC/QTOF-MS) and chemometric analysis (Fig. 1).

Materials and methods

Chemicals and materials

Acetonitrile and formic acid were obtained from Merck (Darmstadt, Germany). Deionized water was purified using a Milli-Q system (Millipore, Bedford, MA, USA). Leucine enkephalin was purchased from Sigma-Aldrich (MO, USA). Carbon tetrachloride (analytical grade) was purchased from Linfeng Chemical Co. (Shanghai, China). *Fructus Ligustri Lucidi* and *Herba Ecliptae* was identified by Professor Qinan Wu of Traditional Chinese Medicine Identification at Nanjing University of Chinese Medicine and purchased from Yonggang Decoction Pieces Co. (Bozhou, Anhui, China). Voucher specimens were deposited at the authors’ laboratory.

Preparation of EZW sample

EZW was prepared as follows: the powder of dry HE (50 g) was immersed in 500 mL of distilled water, decocted by boiling for 1 h and filtered through 16-layers of gauzes. The process above was repeated twice. The extracted solutions were pooled together and concentrated to approximately 0.3 g of HE per milliliter. Finally, the solution was freeze-dried. Before administration, the powder of dry FLL and freeze-dried HE were dissolved in 0.5 % sodium salt of carboxy methyl cellulose (CMC-Na) solution. One milliliter CMC-Na solution contained approximately 0.6 g of FLL and 0.6 g of HE crude drugs, respectively. For the quality control of EZW, four main compounds, nuezhenide, specnuezhenide, wedelolactone, and oleanic acid, were determined by a HPLC-UV system on a C_{18} column [29]. The HPLC-UV method and chromatograms of standards and EZW sample were shown in Figure S3 of Supplemental material. The content of nuezhenide, specnuezhenide, wedelolactone, and oleanic acid were 0.337, 3.582, 0.109, and 11.536 mg/g, respectively. All the index compounds, specnuezhenide, wedelolactone, and oleanic acid in EZW sample for our metabolomics study exceeded the demands of the Pharmacopoeia of the People’s Republic of China, 2010 Edition.

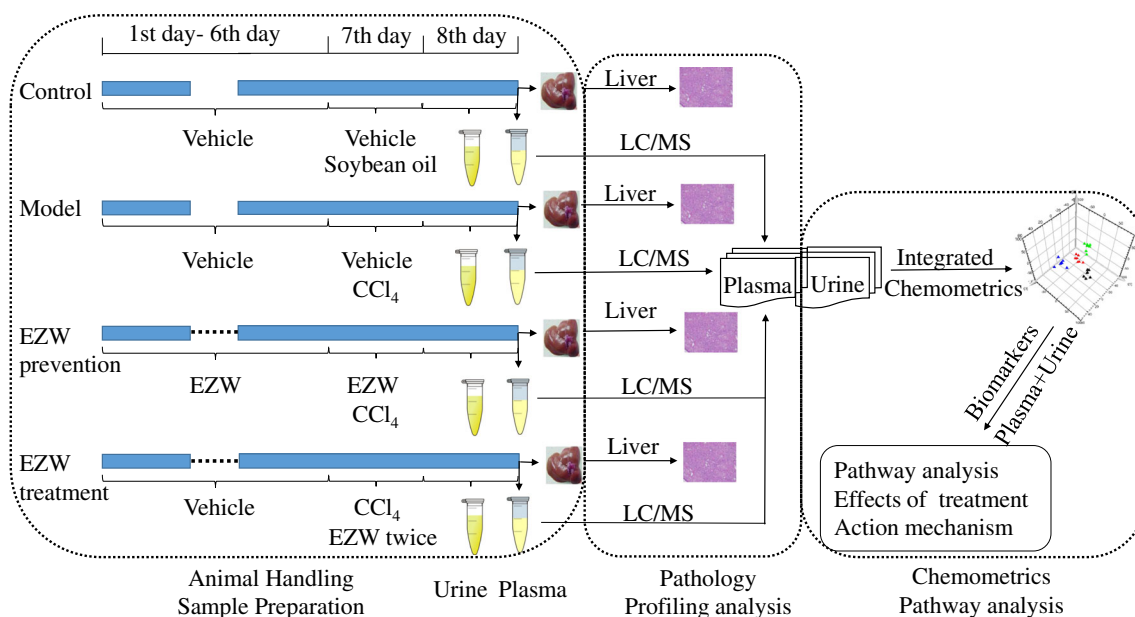


Fig. 1 Overview of the integrated metabolomics strategy. Vehicle, 0.5 % sodium salt of carboxymethyl cellulose (CMC-Na); EZW, FLL and freeze-dried HE were dissolved in 0.5 % CMC-Na solution; CCl₄, 50 % carbon tetrachloride soybean oil solution

Animal handling and sample preparation

Male Wistar rats (weighting 200 ± 20 g) were supplied by the Experimental Animal Center of Nanjing University of Chinese Medicine (Jiangsu, China). Animal welfare and experimental procedures were strictly in accordance with the Guide for the Care and Use of Laboratory Animals (US National Research Council 1996, http://www.nap.edu/openbook.php?record_id=5140&page=R1) and the related ethics regulations of Nanjing University of Chinese Medicine. All animals were fostered in an environmentally controlled breeding room (temperature maintained at about 25 °C and with a 12-h light/12-h dark cycle) for at least 1 week before starting the experiments and fed with standard laboratory food and water ad libitum. All the rats were randomly divided into four groups of seven rats each as follows: control group, model group, EZW-prevented group and EZW-treated group. The EZW-prevented group was orally administrated with EZW solution (1.2 g mL^{-1} , $18 \text{ g kg}^{-1} \text{ day}^{-1}$) for 7 days. Meanwhile, the control, model, and EZW-treated groups were given orally with a volume of 0.5 % CMC-Na solution. After 1 h of the last drug administration, rats in the control group were injected intraperitoneally with soybean oil (1.5 mL kg^{-1}), and the model, EZW-prevented and EZW-treated groups were intraperitoneally injected with 50 % carbon tetrachloride soybean oil solution (1.5 mL kg^{-1}). After 2 h of liver injuring, the EZW-treated group was orally administrated with EZW solution (1.2 g mL^{-1} , $18 \text{ g kg}^{-1} \text{ day}^{-1}$) twice in 12 h. Then, urine was collected for 24 h from metabolism cages at ambient temperature throughout the procedure and centrifuged ($13,000 \text{ r min}^{-1}$) at 5 °C for 15 min. The supernatants were stored frozen at -80 °C for analysis. At the end of 24 h, blood from ophthalmic vein plexus was collected in Eppendorf tube,

diluted with a 10 % disodium-EDTA solution, and centrifuged ($13,000 \text{ r min}^{-1}$) for 10 min. The supernatant, plasma, was stored frozen at -80 °C for metabolomics analysis. Lastly, the liver tissue was cut for pathological section diagnosis and electron microscopic observation.

Metabolic profiling

Plasma metabolite profiling

Frozen plasma samples were thawed and the protein in 200 μL of plasma was precipitated by adding 600 μL methanol. The solutions were centrifuged at $13,000 \text{ r min}^{-1}$ for 10 min. The resulting supernatants were dried under vacuum and reconstituted in 0.2 mL acetonitrile/water (80:20). The solution was then filtered by 0.25 μm membrane for injection. A pooled sample, which was a mixture of small random volumes from all 28 samples, was extracted in the same procedure as above. This sample was used as quality control (QC) and analyzed before or after every seven samples. Two microliters of filtrate was analyzed by an Agilent 6520 HPLC-QTOF system (Agilent Technologies, Santa Clara, CA) consisting of an Agilent 1200 SL liquid chromatograph coupled with a time-of-flight (TOF) mass spectrometer. An Agilent Poroshell 120 EC-C18 column ($2.1 \times 100 \text{ mm}$, $2.1 \mu\text{m}$) with a binary solvent system (solvent A: water with 0.1 % formic acid and solvent B: 0.1 % formic acid in acetonitrile) was utilized. The gradient conditions were linear at 5–60 % B over 0–15 min, 60–90 % B over 15–30 min, and 90–100 % B over 30–40 min. The flow rate was 0.35 mL min^{-1} and the column temperature was maintained at 30 °C. Electrospray ionization (ESI) was used in positive mode. The MS interface capillary

was maintained at 350 °C, with a sheath gas flow of 8 L min⁻¹. The spray voltage for positive ion injection was 4.0 kV. The instrument was scanned over a range of 50–1700 *m/z*. Agilent MassHunter Workstation LC-TOF and QTOF Acquisition software (B.02.01) was used for data acquisition. The typical total ion chromatograms of plasma of four groups were shown in Fig. S1 in the Electronic Supplementary Material (ESM).

Urinary metabolite profiling

Frozen urine samples were thawed, and 500 µl of methanol was added to 500 µl urine. The solutions were centrifuged at 13,000 rpm for 10 min. The resulting supernatants were filtered by 0.25 µm membrane for further analysis. A pooled sample, which was a mixture of small random volumes from all 28 samples, was processed in the same procedure as above. This sample was used as quality control and analyzed before or after every seven samples. LC/MS analysis was performed by the same Agilent 6520 HPLC/QTOF-MS system. The samples were gradient-eluted at 0.35 mL min⁻¹ using (A) 0.1 % formic acid in water and (B) 0.1 % formic acid in acetonitrile (10 % B to 30 % B over 0–5 min, 30 % B to 50 % B over 5–8 min, 50 % B to 60 % B over 8–10 min, 60 % B to 90 % B over 10–13 min). A 5-µL sample aliquot was injected onto a 2.1 × 100 mm Agilent Poroshell 120 EC-C8 2.7 µm particle column heated to 30 °C. Electrospray ionization (ESI) was used in positive mode. The MS interface capillary was maintained at 350 °C, with a sheath gas flow of 8 L min⁻¹. The spray voltage for positive ion injection was 4.0 kV. The instrument was scanned over a range of 50–1700 *m/z*. Agilent MassHunter Workstation LC-TOF and QTOF Acquisition software (B.02.01) was used for data acquisition. The typical total ion chromatograms of urine of four groups were shown in ESM Fig. S2.

Pathological evaluation

After the blood and urine collection, rats were euthanized and portions of liver were harvested for pathological evaluation. The liver portions were subsequently embedded in paraffin wax and stained with H&E, after which pathological analysis was carried out to assess steatosis, inflammation, and necrosis via light microscopy (Olympus, Japan). Liver pathology was evaluated as described by Nanjiet al [30].

Multivariate data analysis and data processing

All chromatographic data from plasma and urine were processed in the same manner by the freely available software package MZmine 2.20 (<http://mzmine.sourceforge.net/>), which performed peak seeking in an automated and unbiased way using *mzdata* file from Agilent MassHunter Workstation Data Acquisition. MZmine 2.20 was used for

peak noise removal, peak detection, and alignment. The intensity of each ion was normalized with respect to the total ion count to generate a data matrix that consisted of the retention time, *m/z* value, and the normalized peak area. The parameters of MZmine 2.20 in this study are listed in ESM Table S1.

An overview about the similarity between the data sets can be obtained by calculating their correlation. Matrix correlation is a generalization of variable correlation, and several matrix correlation methods exist [31]. To illustrate the overlap degree of the plasma and urine LC/QTOF-MS data, the random variables (RV) coefficient [32] is the most appropriate for the current situation [33], because it is orientation-independent and easily calculated from the data. LC/QTOF-MS datasets were the *m*-by-*n* matrices (*m* the number of samples; *n* the number of ion peaks) containing values of ion peak area at different retention time and/or *m/z*. However, directly applying such modality on crude data would result in spurious results due to the high dimensionality of the LC/QTOF-MS datasets. Therefore, a dimension reduction using principal component analysis (PCA) was performed to reduce the unnecessary information of the data sets. After that, the RV coefficient was calculated to measure the degree of overlap between matrices.

One of the goals in metabolomics area of research is to use data obtained from your samples to build an appropriate model for classification and determine the factors leading to differences among the samples. PCA and PLS-DA are often used for this purpose, as these techniques determine orthogonal latent variables that describe the input data and classify the data based on these variables [34]. PCA applied on matrix *X*—the objective is to recover the total variance from all datasets, but the presence of groups (products) in the data is not explicitly taken into account in the computation of the principal components. Partial least squares (PLS) is a particularly useful algorithm. Simply put, PLS is an extension of PCA, a non-supervised method to maximizing variance explained in *X*, which instead maximizes the covariance between *X* and *Y* (s). Before multivariate data analysis, ANOVA in Matlab software version 6.5 was used to eliminate the non-significant variables with the *p* value > 0.05 for the plasma and urine data sets, respectively. For a straightforward and convenient explanation of metabolites, the LC/QTOF-MS data of plasma and urine from the same rat were simply concatenated and processed as a single data set. Then, the combined data set was exported into SIMCA-P software 11.5 (Umetrics AB, Umeå, Sweden) for projections to latent structures discriminate analysis (PLS-DA). Since the scale of metabolite concentrations may be different between plasma and urine, the unit variance (UV) scaling was selected to preprocess the data prior to PLS-DA and leave 1/7 out cross validation was used to determine the optimal model. The purpose of PLS-DA was to calculate models that differentiate between groups or

classes. In the PLS-DA modeling, the samples from different groups were sorted into different classes using score plots, and endogenous metabolites that contribute to the classification were found by variable importance in the projection (VIP) values, which showed the importance of each variable to the classification. For measuring the quality of clustering within a PLS-DA scores plot, the degree-of-class-separation (DCS) was calculated between four groups, which was defined as the class-to-class variance divided by the sum of the within class variance on a scores plot using two sample types in the training set [35].

Biomarker identification and metabolic pathway analysis

With regard to the identification of biomarkers, the ion spectrum was matched with the structure message of metabolites acquired from available biochemical databases, such as METLIN (<http://www.metlin.scipps.edu/>) [36], HMDB (<http://www.hmdb.ca/>) [37] and KEGG (<http://www.genome.jp/kegg/>) [38]. The pathway analysis of potential biomarkers was performed with MetPA software based on the pathway library of *Rattus norvegicus* (rat) to identify the metabolic pathways. MetPA is now part of MetaboAnalyst (<http://www.metaboanalyst.ca/MetaboAnalyst/faces/Home.jsp>) [39].

Results and discussion

Pathological study

Figure 2 shows the representative pathological slices of rat livers from the control group (a), model group (b), EZW-prevented group (c), and EZW-treated group (d). Typical pathological characteristics of liver injury, such as swollen endothelial cells and thickened endomembrane were observed in CCl₄-treated rats (Fig. 2b). For EZW-prevented group and EZW-treated group, similar pathological features of liver injury were still observed; however, these symptoms were less obvious (Fig. 2c, d). Additionally, compared to EZW-treated group, the protective function of EZW was better in EZW-prevented group. The above phenomena indicated that the artificial modeling of liver injury in rats was successful and that the pathological condition was improved with administration of EZW.

The correlation between plasma and urine metabolomics datasets

The RV coefficient takes values between 0 (no overlap) and 1 (total overlap), measuring the closeness of two data set that may each be represented in a matrix. After mean centering, PCA was used to reduce the dimension of plasma and urine

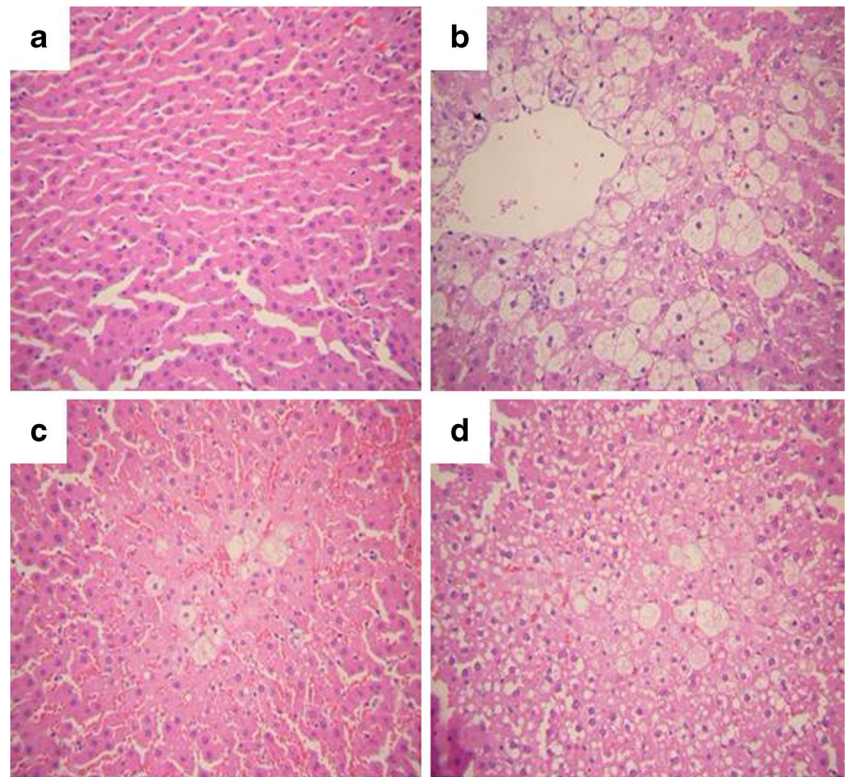
data matrices. Then, the RV coefficient was calculated to measure the degree of overlap (Table 1). The cumulative amounts of explained variation of the principal components in both plasma and urine matrices are larger than 90 % for six to ten principal components, representing the major information in the data sets. After the first seven components, the RV coefficient is 0.26, and it is constant for more components. This means that there is an overlap between the plasma and urine data sets. Hence, it is helpful to combine these two data sets.

Chemometric analysis with plasma and urine metabolomics data

As a first step in chemometric analysis, PCA, an unsupervised multivariate data analysis technique, was performed to visualize grouping trends and outliers in data. Principal component 1 versus principal component 2 score plots of the plasma and urine data are shown in Fig. 3a, b, respectively. The QC samples clustered tightly in both score plots, illustrating the stability of the LC/MS platform throughout the analysis. To reflect the metabolite difference among control, EZW-prevented, EZW-treated, and model groups along with the efficacies of EZW against the liver injury, PLS-DA was employed to construct the model where the variable matrix was made up of LC/MS ion peak areas of plasma and urine metabolite. Generally, the quality of PLS model was evaluated by the relevant R^2X (the cumulative fraction of sum of squares of X explained by components), R^2Y (the cumulative sum of squares of all the y -variables explained by the extracted components), and Q^2Y (the fraction of the total variation of Y (PLS) that can be predicted by the extracted components). Without a high R^2Y , it is impossible to obtain a high Q^2Y . A $Q^2Y > 0.5$ is regarded as good and a $Q^2Y > 0.9$ as excellent, but these guidelines are of course heavily application dependent. Differences between R^2Y and Q^2Y larger than 0.2~0.3 indicate the presence of many irrelevant model terms or a few outlying data points [40]. Different data pretreatment methods, i.e., centering, autoscaling, and Pareto-scaling, were found to greatly affect the outcome of the data analysis and thus the rank, from a biological point of view, of the most important metabolites [41]. The data pretreatment methods used prior to data analysis were tested in our study (see ESM Table S2), and the “UV (autoscaling)” was selected for further PLS-DA.

As shown in Table 2, the values of R^2X , R^2Y , and Q^2Y were also acceptable for single plasma or urine data sets, but the combination of two data sets supplied better results ($R^2Y=0.985$, $Q^2Y=0.937$), indicating an excellent prediction. Compare to the result before ANOVA, the lower latent variable number and the lower difference (0.048) between R^2Y and Q^2Y further make the analysis stable and confident. The compared performances of PLS-DA are shown in the 3D-score plots (Fig. 4). In Fig. 4A,

Fig. 2 Pathological photographs of rat livers (H & E, $\times 100$). **a** Control; **b** Model; **c** EZW-prevented; **d** EZW-treated



B, the single source of metabolomics data, plasma, or urine, could not make the border obvious among the four groups. In the same direction, the distribution among four groups was more obvious for the combined plasma and urine data sets (Fig. 4c), suggesting the more discriminant information from the integrated metabolomics data. In this work, the quantitative index, DCS, on the PLS-DA scores

plot was also calculated between different groups from the integrated and single data sets (see ESM Table S3–S5). For the integrated plasma and urine data, the DCS between Control and Model groups was 10.5617, it was 12.2244 between Control and EZW-prevented groups, and it was 8.6144 between Control and EZW-treated groups. This metric was 9.4230 between Model and

Table 1 Correlation between the plasma and urine metabolomics data matrices

PCs ^a	Plasma (%)		Urine (%)		RV ^d
	Variance ^b	Cumulative variance ^c	Variance	Cumulative variance	
1	42.93	42.93	45.41	45.41	0.0189
2	35.51	78.44	26.50	71.91	0.2022
3	8.05	86.49	12.11	84.02	0.2324
4	3.42	89.91	5.21	89.23	0.2455
5	3.02	92.93	2.09	91.32	0.2525
6	1.73	94.66	1.47	92.80	0.2564
7	1.62	96.28	1.06	93.87	0.2615
8	0.78	97.06	0.85	94.72	0.2639
9	0.68	97.74	0.77	95.50	0.2646
10	0.62	98.36	0.67	96.16	0.2656

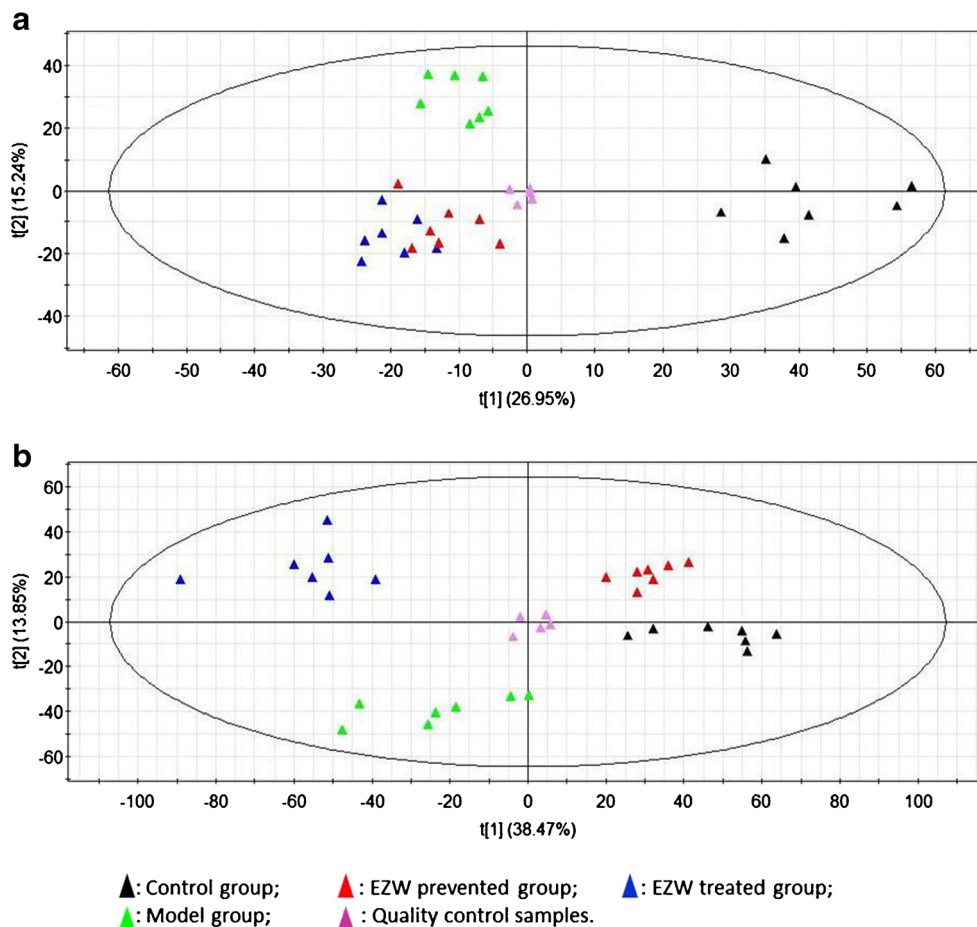
^aPCs principal components

^bThe percentage of explained variance for each PC

^cThe cumulative percentage of explained variance

^dThe RV coefficient: a matrix correlation coefficient

Fig. 3 The score plots of principal components analysis. (a) plasma, $R^2X=0.645$, $Q^2=0.395$; (b) urine, $R^2X=0.778$, $Q^2=0.584$



EZW-prevented groups and 6.2819 between Model and EZW-treated groups. Most of the DCS values showed how much better can PLS-DA cluster the different groups using the integrated data set than using the single data set. The PCA 3D-score plot (see ESM Fig. S4) and its DCS values (see ESM Table S6) were also compared with those of PLS-DA's, and we can find less DCS values and worse separation.

Table 2 Summary of PLS-DA

Profiles	A^a	R^2X	R^2Y	Q^2Y	Difference ^b
Plasma	8	0.883	0.973	0.870	0.103
Plasma ^c	5	0.719	0.917	0.812	0.105
Urine	7	0.725	0.979	0.880	0.099
Urine ^c	4	0.629	0.935	0.875	0.060
Plasma+urine	7	0.700	0.981	0.913	0.068
Plasma+urine ^c	6	0.672	0.985	0.937	0.048

^a The number of latent variables

^b The difference between R^2Y and Q^2Y

^c The data after ANOVA

Tentative identification of the biomarkers and pathway analysis

The PLS-DA model built above simultaneously considers the plasma and urine metabolomic profiles, and then variable selection is brought forth as the important practical issues for metabolomics. The data set was screened with a VIP value larger than 1.0 for further metabolite identification. Seven potential biomarkers are summarized in Table 3 with their corresponding retention time, m/z , formula, adduct ion, trends, and related metabolic pathways. Differentially expressed metabolites were pipecolic acid, tryptophan, sphinganine, and tetrahydrocorticosterone in plasma. In addition, pipecolic acid, L-2-amino-3-oxobutanoic acid, and phosphoribosyl pyrophosphate were significant metabolites in urine. All of them have the direction of perturbation (up- or downregulation) in the four groups. They could be considered as potential markers for biological pathway analysis. Compared with other multiplatform metabolomics data analysis [42, 43], it has indicated that a better discriminate model could be built with the integrated plasma and urine data from the separation of different groups in Fig. 4 and the DCS values. This data processing of combination could help us to search the most

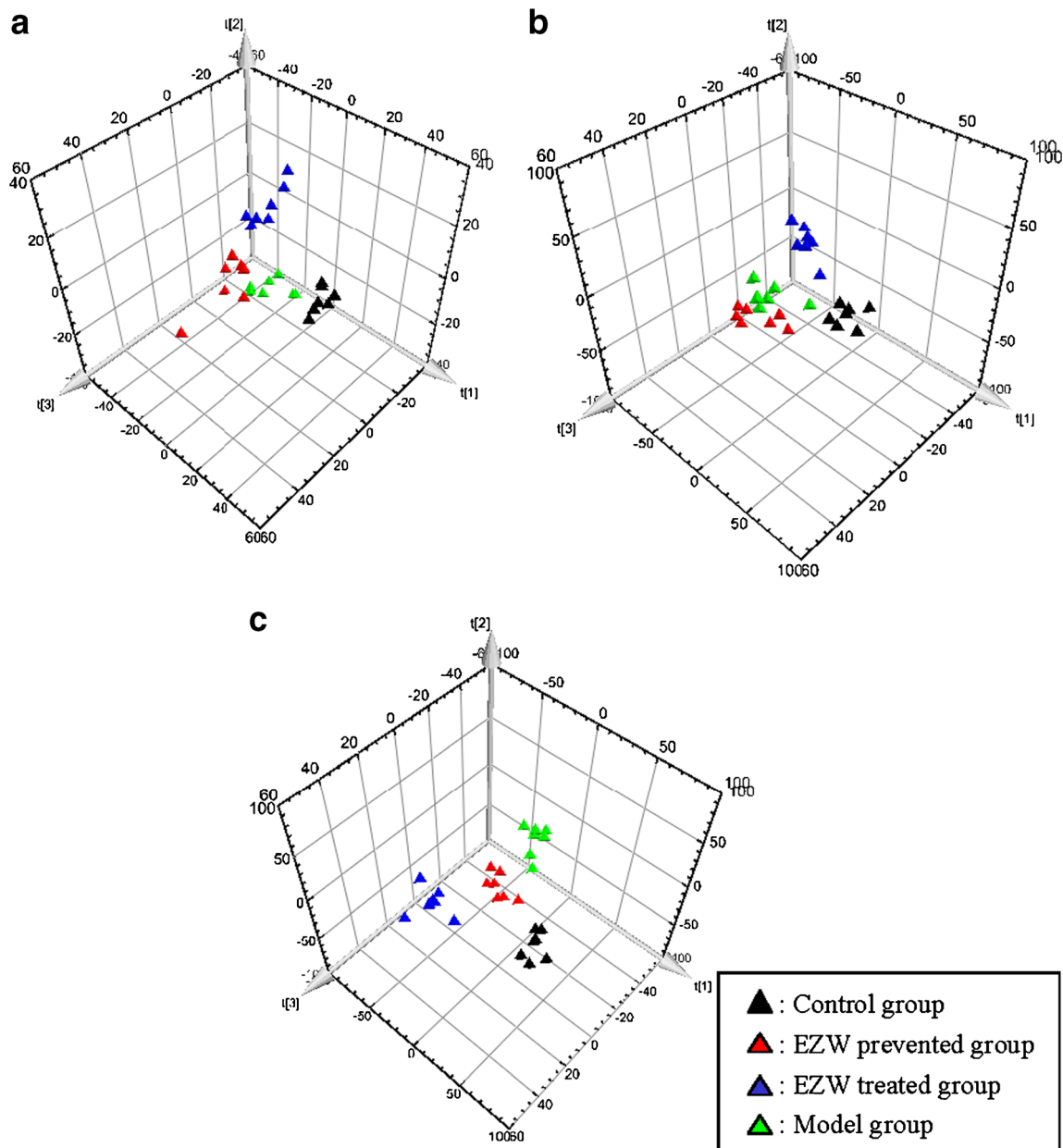


Fig. 4 The 3D score plot (t1/t2/t3) of PLS. (a) plasma, $R^2X=0.719$, $R^2Y=0.917$, $Q^2Y=0.812$; (b) urine, $R^2X=0.629$, $R^2Y=0.935$, $Q^2Y=0.875$; (c) plasma+urine, $R^2X=0.672$, $R^2Y=0.985$, $Q^2Y=0.937$

significant biomarkers in the samples according to the best model. And an important biomarker, pipecolic acid, has been detected in both plasma and urine, which really exists in the above two kinds of samples [44].

Metabolite profiling focuses on the analysis of a group of metabolites related to a specific metabolic pathway in biological states [45, 46]. To determine whether our observations of changes in the metabolites in the setting of liver injury in fact reflected coordinate changes in defined metabolic pathways, we used the pathway library of *R. norvegicus* (rat) in MetPA software to identify the most relevant pathways involved in the conditions under study. Six metabolic pathways,

tryptophan metabolism, sphingolipid metabolism, steroid hormone biosynthesis, lysine degradation, glycine, serine and threonine metabolism, and pentose phosphate pathway, were identified (Table 3).

Effects of EZW on the metabolic pathway

The changed concentrations of potential biomarkers (Table 3) suggested that the disturbed pathways in liver injury rats, such as tryptophan metabolism, sphingolipid metabolism, steroid hormone biosynthesis, lysine degradation, glycine, serine and threonine metabolism, and pentose phosphate pathway, were

Table 3 Potential biomarkers and their metabolic pathways in the pathway library of *Rattus norvegicus*

Matrix	No	R.T.(min)	Mass (<i>m/z</i>)	Adduct ion	Delta	Formula	Compound	Trend ^a	Trend ^b	Trend ^c	Related pathways
Plasma	1	1.218	130.0856	M+H	0.0006	C ₆ H ₁₁ NO ₂	Pipecolic acid	↑	↓	↓	Lysine degradation
	2	2.6	227.0788	M+Na	0.0002	C ₁₁ H ₁₂ N ₂ O ₂	L-Tryptophan	↓	↑	↑	Tryptophan metabolism
	3	9.427	340.2613	M+K	0.0001	C ₁₈ H ₃₉ NO ₂	Sphinganine	↓	↑	↑	Sphingolipid metabolism
	4	9.576	351.2525	M+H	0.0005	C ₂₁ H ₃₄ O ₄	Tetrahydrocorticosterone	↑	↓	↓	Steroid hormone biosynthesis
Urine	1	0.712	130.0874	M+H	0.0011	C ₆ H ₁₁ NO ₂	Pipecolic acid	↑	↓	↓	Lysine degradation
	2	0.845	140.0263	M+Na	0.0055	C ₄ H ₇ NO ₃	L-2-Amino-3-oxobutanoic acid	↑	↓	↓	Glycine, serine and threonine metabolism
	3	10.22	390.9554	M+H	0.0037	C ₅ H ₁₃ O ₁₄ P ₃	Phosphoribosyl pyrophosphate	↑	↓	↓	Pentose phosphate pathway

^a ↑ or ↓ represents the up- or downregulation of the metabolites in model group compared with the control group

^b ↑ or ↓ represents the significant up- or downregulation of the metabolites in EZW-prevented group compared with the model group

^c ↑ or ↓ represents the significant up- or downregulation of the metabolites in EZW-treated group compared with the model group

affected by the administration of EZW. According to the PLS score plot (Fig. 4), the metabolic patterns of the rats subjected to control, EZW-prevented, EZW-treated, and model groups were not discriminated visibly with the single plasma or urine dataset. The result of integrated data showed clear separation in the PLS score plot (Fig. 4c), indicating the existence of differences among four groups. In order to further demonstrate the action of EZW, the PLS score plot (t2 versus t3) was shown in Fig. 5. Compared to the model group, the EZW-prevented, control, and EZW-treated groups were situated at the same level in the score plot, indicating the recovery of body to some extent after the administration of EZW.

Here, the important plasma and urine biomarkers associated with liver injury and EZW-treated modulation were analyzed in these pathways (Fig. 6). Tryptophan is an essential amino acid in the tryptophan metabolism. Amino acids, including tryptophan, act as building blocks in protein biosynthesis through the action of tryptophanyl tRNA synthetase. This metabolite demonstrated that abnormal metabolism occurred in the model animals and metabolic analysis of liver injury was inferred from changes in the intermediates during substance metabolism [47].

In sphingolipids metabolism, sphinganine is ubiquitous but essential structural and functional components of the cell. As a

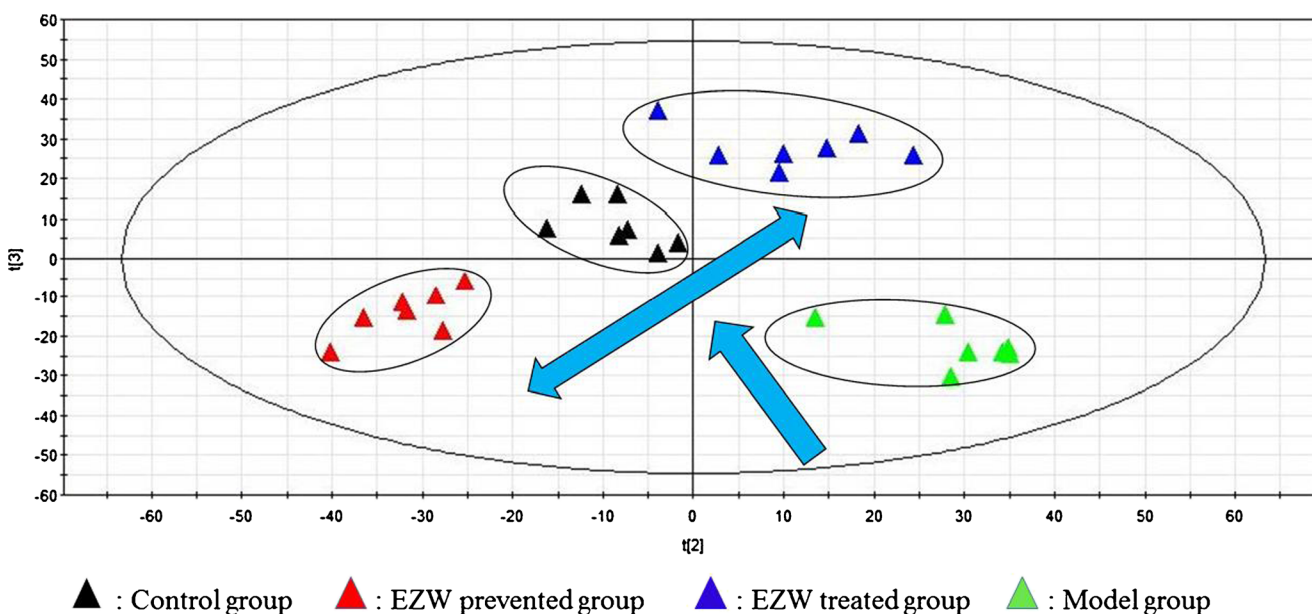
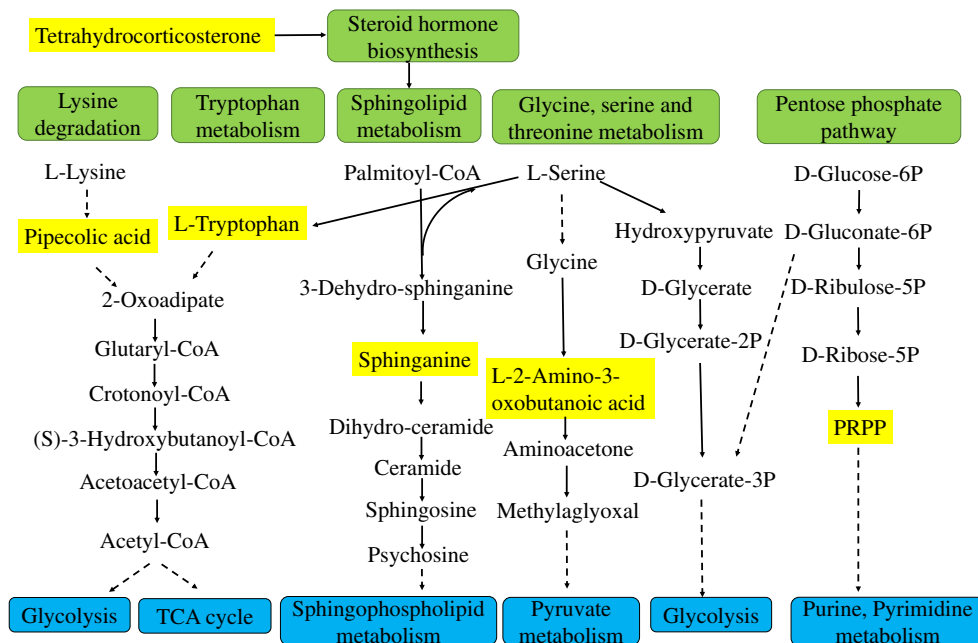


Fig. 5 The PLS-DA scores (t2/t3) plot of integrated plasma and urine data. $R^2X[2]=0.161$, $R^2X[3]=0.119$

Fig. 6 The network of the potential biomarkers changing for liver injury and EZW-treated modulation. Metabolites in yellow boxes represent biomarkers determined by LC/QTOF-MS. The green boxes represent the pathway related to the liver injury. The blue boxes are the possible pathways succeeded. PRPP phosphoribosyl pyrophosphate



sphingolipid metabolite, sphinganine-1-phosphate is produced by the ATP-dependent phosphorylation of sphinganine by sphingosine kinases 2 in sphingolipid metabolism. It has important biological roles in various physiological as well as pathophysiological events. Recently, sphinganine-1-phosphate has been reported to protect against both liver and kidney injury [48]. In this study, the decreased concentration of sphinganine in the model group indicates that the CCl₄-injured rats might lose the protection of normal metabolite. Tetrahydrocorticosterone is the compound in the steroid hormone biosynthesis. Recently, Lucki [49] has discussed how steroid hormones control sphingolipid metabolism and sphingolipids, including ceramide, sphingosine-1-phosphate, and sphingosine, have been found to modulate steroid hormone secretion at multiple levels. Hence, tetrahydrocorticosterone might indirectly affect the liver protection function of the sphinganine-1-phosphate through the steroid hormone biosynthesis. By the prevented or treated administration of EZW, the concentrations of sphinganine and tetrahydrocorticosterone were recovered, and the liver of rats could be protected again.

In lysine degradation, pipecolic acid is a metabolite of lysine found in physiological fluids such as urine and plasma [50]. It was found by Fujita [44] that both D-pipecolic acid and L-pipecolic acid were moderately increased in patients with liver cirrhosis and in patients with chronic hepatic encephalopathy. Although L-pipecolic acid remained the predominantly circulating form, D-pipecolic acid was proportionally higher in liver disease patients than in healthy individuals. Patients with liver cirrhosis have elevated levels of GABA and pipecolic acid in plasma [51]. And plasma pipecolic acid is closely correlated with plasma ammonia concentration. This

work also revealed that the degree of portal hypertension in cirrhotic patients may be predicted by plasma pipecolic acid. In our study, the concentration of pipecolic acid is increased in the model group and the EZW help the pipecolic acid levels in both plasma and urine to increase, indicating the recovery of liver function.

Phosphoribosyl pyrophosphate is a pentose phosphate from the pentose phosphate pathway. The pentose phosphate pathway in animals fulfills two important cell requirements: (1) for ribose 5-phosphate for the synthesis of nucleotides and nucleic acids; and (2) for reducing power in the form of NADPH. In photosynthesis, it functions to regenerate the primary CO₂ acceptor, ribulose bisphosphate, from the hexose phosphates produced [52]. Chloroplasts utilize radiant energy to produce ATP, required for the production of ribulose 1,5-bisphosphate from ribulose 5-phosphate and also for the reduction of 3-phosphoglyceric acid to glyceraldehyde 3-phosphate. Some research results also appear to demonstrate that phosphoribosyl pyrophosphate bioavailability in liver as a key compound is most closely controlled by the energy charge [53]. The concentration of phosphoribosyl pyrophosphate increases in the model group, indicating some disorder in liver and then it is decreasing in EZW-prevented and treated groups.

Conclusion

A robust integrated metabolomics approach utilizing HPLC/QTOF-MS was developed to investigate the influence of Er-Zhi-Wan on the CCl₄ liver-injured rats. Pattern

recognition analysis allowed the metabolic profiles of control, EZW-prevented, EZW-treated, and model groups to be separated clearly, indicating a more comprehensive information from integrated information. Six potential biomarkers were identified from plasma and urine specimens. According to the pathway library of *R. norvegicus* (rat), six metabolic pathways were disturbed among groups, relating to tryptophan metabolism, sphingolipid metabolism, steroid hormone biosynthesis, lysine degradation, glycine, serine and threonine metabolism, and pentose phosphate pathway. The combination of plasma and urine metabolomics provides a powerful means of revealing changes in the metabolome due to liver injury and EZW efficacy. The presented metabolomics strategy could be extended to other multiple-source metabolomics studies, e.g., different analytical platforms, different omics or different specimens. Certainly, for quantitatively investigating effect of EZW for liver injury, these biomarkers should be determined more accurately. The quantitative analysis of biomarkers should be done in a further study to characterize the effects of traditional Chinese medicine to prevent liver injury and protect the liver.

Acknowledgments This work was financially supported by National Natural Science Foundation of China (Grant No. 81001599, 81173547, and 81373972) and A Project Funded by the Priority Academic Program Development of Jiangsu Higher Education Institutions (PAPD).

References

- Griffin JL, Walker LA, Garrod S, Holmes E, Shore RF, Nicholson JK (2000) *Comp Biochem Physiol, Part B: Biochem Mol Biol* 127:357–367
- Irie M, Fujimura Y, Yamato M, Miura D, Wariishi H (2014) *Metabolomics* 10:473–483
- Li M, Li H, Jiang P, Liu XQ, Xu D, Wang F (2014) *Mol BioSyst* 10:1055–1062
- Zhao XJ, Zhang Y, Meng XL, Yin PY, Deng C, Chen J, Wang Z, Xu GW (2008) *J Chromatogr B Anal Technol Biomed Life Sci* 873:151–158
- Antti H, Ebbels TMD, Keun HC, Bollard ME, Beckonert O, Lindon JC, Nicholson JK, Holmes E (2004) *Chemom Intell Lab Syst* 73:139–149
- Beyoğlu D, Idle JR (2013) *J Hepatol* 59(4):842–858
- Qiu J (2007) *Nature* 448:126–128
- Qiu J (2007) *Nat Rev Drug Discov* 6:506–507
- Wang M, Lamers RJ, Korthout HJ (2005) *Phytother Res* 19:173–182
- Gou X, Tao Q, Feng Q, Peng J, Sun S, Cao H (2013) *J Pharm Biomed Anal* 74:62–65
- The National Pharmacopoeia Commission of P.R. China (2010) *Pharmacopoeia of the People's Republic of China, vol. 1. Chinese Medical Science and Technology Press, Beijing*, pp 412–413
- Zhang AH, Sun H, Dou SS, Sun WJ, Wu XH, Wang P, Wang XJ (2013) *Analyst* 138:353–361
- Cai XJ, Yan B, Yao WF, Zhang L, Huang MY, Ding AW (2011) *Chinese Pharmacological Bull* 27(12):1774–1775
- Gao HL, Wang DQ, Wang XY (2010) *Chin J Integr Med* 16(6):504–509
- Xu H, Su ZR, Huang W, Choi RC, Zheng YZ, Lau DT, Dong TT, Wang ZT, Tsim KW (2012) *J Ethnopharmacol* 143(1):109–115
- Yan B, Cai XJ, Yao WF, Zhang L, Huang MY, Ding AW (2012) *China J Chin Mater Med* 37(9):1303–1305
- Zhen C, Lifu S, Jinhong H, Qian S (1998) *Acad J Sec Mil Med Univ* 19(1):76–78
- Kobori M, Yang Z, Gong D, Heissmeyer V, Zhu H, Jung YK, Gakidis MAM, Rao A, Sekine T, Ikegami F, Yuan C, Yuan J (2004) *Cell Death Differ* 11(1):123–130
- Han DW, Ma XH, Zhao YC, Yin L, Ji CX (1982) *J Tradit Chin Med* 2(2):83–90
- Liu J (2005) *J Ethnopharmacol* 100(1–2):92–94
- Liu J, Liu Y, Klaassen CD (1994) *J Ethnopharmacol* 42(3):183–191
- Liu J, Liu Y, Parkinson A, Klaassen CD (1995) *J Pharmacol Exp Ther* 275(2):768–774
- Cheng M, Wang QW, Fan YK, Liu XY, Wang L, Xie RM, Ho CC, Sun WJ (2011) *J Ethnopharmacol* 138(2):279–285
- Shimada T, Nakanishi T, Toyama A, Yamauchi S, Kanzaki A, Fujiwake H, Sato TA, Ikegawa M (2010) *J Proteome Res* 9(9):4490–4500
- Henkel C, Roderfeld M, Weiskirchen R, Berres ML, Hillebrandt S, Lammert F, Meyer HE, Stühler K, Graf J, Roeb E (2006) *Proteomics* 6(24):6538–6548
- Atmaca M, Bilgin HM, Obay BD, Diken H, Kelle M, Kale E (2011) *J Physiol Biochem* 67(4):569–576
- van Ginneken V, Verhey E, Poelmann R, Ramakers R, van Dijk KW, Ham L (2007) *Biochim Biophys Acta* 1771:1263–1270
- Garcia-Canaveras JC, Donato MT, Castell JV, Lahoz A (2011) *J Proteome Res* 10:4825–4834
- He M, Yao WF, Zhang L, Ding AW (2012) *Zhongguo Zhong Yao Za Zhi* 37(5):594–596
- Nanji AA, Mendenhall CL, French SW (1989) *Clin Exp Res* 13(1):15–19
- Ramsay JO, Ten Berge JMF, Styanc GPH (1984) *Psychometrika* 49:403–423
- Robert P, Escoufier Y (1976) *Appl Stat* 25:257–265
- Smilde AK, Westerhuis JA, De Jong S (2003) *J Chemom* 17:323–337
- Eriksson L, Johansson E, Kettaneh N, Trygg J, Wikstrom C, Wold S (2006) *Multivariate and megavariate data analysis part I: basic principles and applications, second revised and enlarged edition*. Sweden, Umetrics Academy, p 189
- Pierce KM, Hope JL, Johnson KJ, Wright BW, Synovec RE (2005) *J Chromatogr A* 1096:101–110
- Smith CA, O'Maille G, Want EJ, Qin C, Trauger SA, Brandon TR, Custodio DE, Abagyan R, Siuzdak G (2005) *Ther Drug Monit* 27(6):747–751
- Wishart DS, Tzur D, Knox C. (2007) *Nucleic Acids Res. (Database issue): D521-526*.
- Kanehisa M (2002) *Novartis Found Symp* 247:91–101
- Xia J, Mandal R, Sinelnikov IV, Broadhurst D, Wishart DS (2012) *Nucleic Acids Res.* 40(Web Server issue): W127-33.
- Eriksson L, Johansson E, Kettaneh N, Trygg J, Wikstrom C, Wold S (2006) *Multivariate and megavariate data analysis part I: basic principles and applications, second revised and enlarged edition*. Umetrics Academy, Sweden, p 97
- Van den Berg R, Hoefstloot H CJ, Westerhuis J, Smilde A, van der Werf MJ (2006) *BMC Genomics* 7:142
- Huang Y, Tian Y, Li G, Li Y, Yin X, Peng C, Xu F, Zhang Z (2013) *Anal Bioanal Chem* 405:4811–4822
- Zhang H, Fu P, Ke B, Wang S, Li M, Han L, Peng C, Zhang W, Liu R (2014) *J Ethnopharmacol* 154(1):55–64
- Fujita T, Hada T, Higashino K (1999) *Clin Chim Acta* 287:145–156
- Musiek ES, Yin H, Milne GL, Morrow JD (2005) *Lipids* 40(10):987–994

46. Cho HJ, Kim JD, Lee WY, Chung BC, Choi MH (2009) *Anal Chim Acta* 632(1):101–108
47. Zhang AH, Sun H, Sun WJ, Jiao GZ, Wang XJ (2013) *Anal Methods* 5:5294–5301
48. Park SW, Kim M, Chen SW, Brown KM, D'Agati VD, Lee HT (2010) *Lab Investig* 90(8):1209–1224
49. Natasha CL, Marion BS (2010) *Steroids* 75(6):390–399
50. Fujita T, Amuro Y, Hada T, Higashino K (1999) *Clin Chim Acta* 287(1–2):99–109
51. Matsuda Y, Fujita T, Hada T, Higashino K (2000) *Hepato Res* 18(2):132–140
52. Bernard LH (2002) *J Biol Chem* 277(50):47965–47971
53. Kunjara MS, Ali SA, Greenbaum AL, McLean P (1987) *Biochem J* 244:101–108